American Mineralogist, Volume 73, pages 62–76, 1988

Compositional and structural variations of phyllosilicates from the Point Sal ophiolite, California

LORI A. BETTISON, PETER SCHIFFMAN
Department of Geology, University of California, Davis, California 95616, U.S.A.

ABSTRACT

Detailed analytical studies of mafic phyllosilicates from volcanic and hypabyssal intrusive rocks from the upper portion of the Point Sal remnant of the California Coast Range ophiolite reveal a notable correlation between phyllosilicate mineral parageneses and ophiolite pseudostratigraphy. Five phyllosilicate phases have been identified by systematic X-ray diffraction studies on clay size fractions: (1) smectite occurs in minor amounts in the upper volcanic zone (1A lavas), (2) randomly mixed-layered chlorite/smectite is ubiquitous in the 1A lavas but less common in the lower volcanic zone (1B lavas), (3) regularly interstratified chlorite/smectite occurs in both volcanic units, (4) chlorite is present in the 1B lavas and dike and sill complex, and (5) celadonite occurs sporadically throughout the 1A lavas. With increase in depth, smectite layers progressively transform to chlorite so that chlorite is the predominant phyllosilicate in the dike and sill complex.

The phyllosilicate zonation correlates with the calc-silicate mineral parageneses. Discrete smectite and randomly interlayered chlorite/smectite occur in both zeolite- and pumpellyite-grade volcanic rocks. Regularly interlayered chlorite/smectite is more common in pumpellyite-grade volcanic rocks than in the zeolite-grade volcanic rocks, but discrete chlorite is restricted to epidote-grade volcanic rocks and dikes/sills. The authigenic mineral zonation at Point Sal is similar to that reported for the Del Puerto ophiolite and from some active geothermal systems.

Phyllosilicates in the Point Sal remnant exhibit compositional trends correlative to pseudostratigraphic depth. The Si content of phyllosilicates decreases with depth from 7.8 to 5.5 cations/28 oxygens because of decrease in smectite interlayers with depth. Ca contents of mixed-layered chlorite/smectite, correlated with presence of smectite, also decrease with depth.

Mafic phyllosilicates from hydrothermally recrystallized metavolcanic rocks exhibit systematic structural and compositional variations. Chlorite from the Coast Range ophiolite, Troodos ophiolite, DSDP Hole 504B, and Onikobe and Icelandic geothermal fields that has been identified with X-ray diffractometry does not have Si cation totals greater than 6.25 cations/28 oxygens. Detailed X-ray diffraction studies of many layer silicates from low-grade metabasaltic rocks, previously identified as chlorite on the basis of compositional information alone, may lead to their re-identification as various interlayered phases.

INTRODUCTION

The relationship between metamorphic grade and pseudostratigraphic depth within ophiolite complexes ordinarily has been delineated by calc-silicate mineral parageneses (see reviews by Moody, 1979; Coleman, 1984; Liou et al., 1987). However, phyllosilicates such as smectite, interlayered chlorite/smectite, and chlorite are abundant in low-grade metabasites. Regularly interlayered chlorite/smectite ("corrensite") and randomly interlayered chlorite/smectite occur as intermediate products of the continuous transformation of smectite into chlorite. The presence of these mixed-layered phases has been documented in burial metamorphic environments (Hoffman and Hower, 1979), active geothermal systems (Kristmannsdóttir, 1975; Keith et al., 1984; Liou et al., 1985), ophiolites (Evarts and Schiffman, 1983), and the oceanic crust (Alt et al., 1986). These phases have also been produced experimentally (Velde, 1977) at temperatures between 300 and 400 °C and pressures of 2 kbar. Both field and experimental studies indicate that the transition from smectite to chlorite is complex and occurs concurrently with calc-silicate mineral transitions from the zeolite to greenschist facies.

Studies of submarine alteration of the Del Puerto ophiolite by Evarts and Schiffman (1983) and Schiffman et al. (1984) represent the only comprehensive investigations of metamorphic mineral paragenesis of a Coast Range ophiolite remnant. The Del Puerto remnant is characterized by increasing grade of metamorphism and decreasing intensity of the alteration downward in the

0003–004X/88/0102–0062$02.00

pseudostratigraphy of the ophiolite. Chloritic phyllosilicates occur throughout most of the ophiolite. Mixed-layered chlorite/smectite was identified in the volcanogenic rocks that overlie the Del Puerto remnant and in the ophiolitic volcanic rocks. "Corrensite," identified by Evarts and Schiffman (1983) as regularly mixed-layered chlorite/smectite, was found in pumpellyite-bearing volcanic rocks. Discrete chlorite is restricted to epidote-grade volcanic rocks.

The mixed-layered mafic phyllosilicates are particularly interesting because the nature of the interlayering appears to be temperature-sensitive (Kristmannsdóttir, 1975, 1979). These phases may therefore be useful index minerals in low-grade metavolcanics. In this study we document the mafic phyllosilicate mineralogy of metavolcanic and metadiabasic rocks of the Point Sal remnant of the California Coast Range ophiolite. Detailed X-ray diffraction and electron-microprobe analyses of phyllosilicate minerals have been performed in order to document systematic changes in physical and chemical properties of phyllosilicate minerals due to low-grade metamorphism of mafic rocks. In this study it will be shown that (1) Point Sal mafic phyllosilicates have compositional and structural properties that vary systematically with increase in metamorphic grade, (2) the observed phyllosilicate zonation correlates with calc-silicate mineral zonation, and (3) Point Sal phyllosilicates are similar to the compositions and zonations of those from the Del Puerto remnant but are higher grade than those found in most ophiolites and oceanic crust.

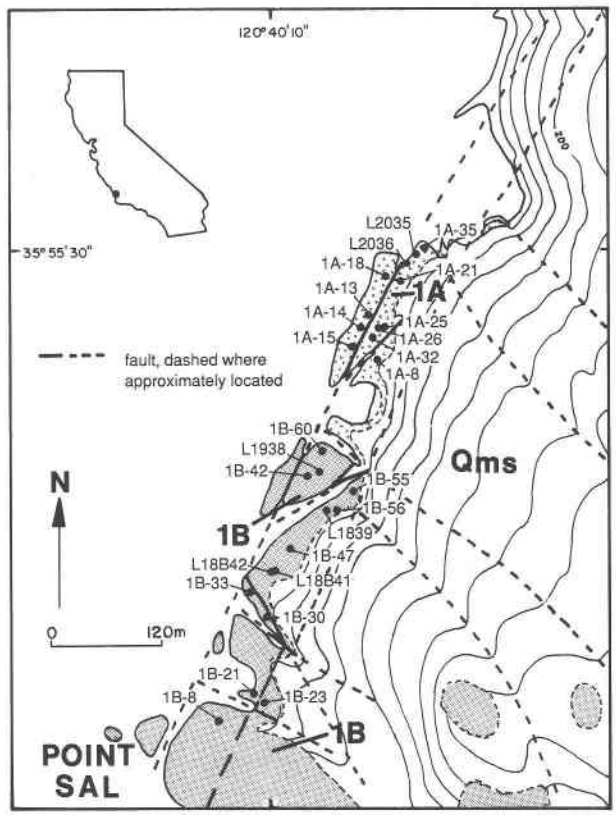

Fig. 1. Geologic map of volcanic units exposed along the coast north of Point Sal with localities of volcanic rocks analyzed in this study. Geologic map adapted from Hopson et al. (1975).

Geologic setting

The Point Sal ophiolite is located approximately 24 km west of Santa Maria, California (Fig. 1), and is one of the twenty-three known remnants of the Jurassic California Coast Range ophiolite (Hopson et al., 1981). Two origins have been suggested for the Coast Range ophiolite: (1) formation at a mid-ocean spreading center (Bailey et al., 1970; Page, 1972; Bailey and Blake, 1974; Pike, 1974; Hopson and Frano, 1977; Hopson et al., 1981) and (2) formation within or near an island-arc setting (Evarts, 1977; Blake and Jones, 1981; Saleeby, 1981; Shervais and Kimbrough, 1985; Evarts and Schiffman, 1983).

The rocks at Point Sal represent a nearly complete 3-km-thick ophiolite sequence that includes pillow lavas, a sheeted dike or sill complex, a plutonic member, and a basal member of harzburgite. The volcanic unit is approximately 1.3 km thick and has been separated by Hopson et al. (1975) into the upper 1A lavas, which contain olivine phenocrysts, and the lower 1B lavas, which lack olivine phenocrysts. The 1A lavas are mostly aphyric to microporphyritic basalts containing clinopyroxene, plagioclase, and olivine phenocrysts. The 1B lavas are aphyric to microporphyritic with clinopyroxene and plagioclase phenocrysts. The dike and sill complex includes felsic, intermediate, and mafic intrusive rocks. The plutonic member consists of dioritic and gabbroic rocks underlain by serpentinized dunite and wehrlite; slivers of serpentinized harzburgite are caught up within the basal fault zone against Miocene Monterey Formation. The entire sequence is comformably overlain by tuffaceous chert of Tithonian age (Hopson et al., 1975).

Methods

Twenty-five samples were chosen from the volcanic units for vertical and lateral variation (Fig. 1), and three were chosen from the dike and sill complex (located south of area shown on map). Thin sections were examined to determine the distribution and textural variation of secondary minerals.

Clay size fractions from whole-rock powders were prepared for X-ray diffraction. Carbonates in the powders were dissolved with a buffered sodium acetate solution and were then centrifuged for removal of the 2-μm size fraction for analysis (Jackson, 1975). Samples were plated onto ceramic tiles composed of quartz and mullite. Two tiles were prepared for each sample, and four analyses of the oriented samples were performed with the following treatments: (1) air dried (Mg-saturated), (2) glycerol solvated, (3) KCl saturated, and (4) heated at 550 °C. The remainder of the material was dried for preparation of an unoriented powder mount. Seven representative clay separates, selected to determine percent chlorite using a method developed by Hower (1981), were plated onto individual tiles and were analyzed after the following treatments: (1) air drying and (2) glycolation using ethylene glycol in a dessicator at 60 °C. A complete description

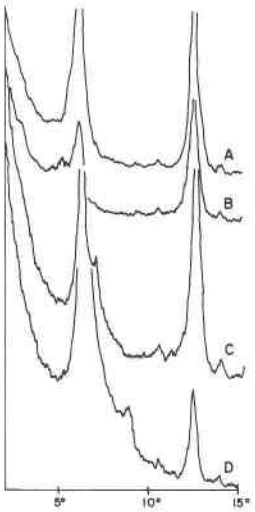

Fig. 2. X-ray pattern of chlorite from sample 1B-56. (A) Mg saturated, (B) glycerol solvated, (C) KCl saturated, (D) heated at 550 °C. This sample also contains minor mixed-layered chlorite/smectite as shown by small reflections at approximately 5° 2θ in B and approximately 8.5° 2θ in D.

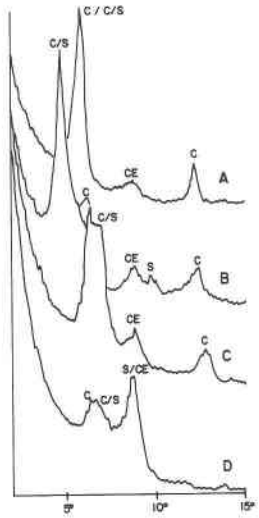

Fig. 3. X-ray pattern of randomly interlayered chlorite/smectite (C/S) from sample 1A-25. This sample also contains discrete chlorite (C), discrete smectite (S), and celadonite (CE). (A) Mg saturated, (B) glycerol solvated, (C) KCl saturated, (D) heated at 550 °C.

of sample-preparation techniques is presented by Bettison (1986). Clay-mineral separates were analyzed on a Diano 8000 X-ray diffractometer using Cu-$K\alpha$ radiation. A graphite monochromator selectively eliminated diffracted Cu-Kβ radiation. Oriented tiles were scanned from 2° to 15° 2θ at 1.6°/min. Unoriented samples were scanned from 59° to 62° 2θ.

Energy-dispersive microprobe analyses of clay minerals within polished thin sections were conducted on an ARL-EMX microprobe equipped with a Kevex 7000 energy-dispersive spectrometer. Analyses were determined using an accelerating voltage of 15 kV, beam current of 100 nA, a beam diameter of 2–3 μm, and counting times of 100–200 s corrected for dead time. Standards used for phyllosilicate analyses included orthoclase (K), albite (Na), cossyrite (Mn, Ti, Fe), synthetic diopside-jadeite glass (Mg, Si), and bytownite (Ca, Al). EDS data were corrected for ZAF effects with the program Magic V (Colby, 1968).

Results

X-ray diffraction analyses

The phyllosilicates identified in the volcanic section and dike and sill complex of the Point Sal ophiolite include smectite, randomly interlayered chlorite/smectite, regularly interlayered chlorite/smectite, chlorite, and celadonite. Identification of smectite, chlorite, and celadonite is generally unambiguous. Smectite, found in 19 of the 34 samples studied, was recognized by the expansion of the (001) spacing from 14 to 17.9 Å with glycerol solvation and collapse to 10 Å with heating at 550 °C. Chlorite is present in all but one of the samples and was identified by the (001) spacing at 14 Å, which is not modified by glycerol solvation and which is not affected by heat treatments at temperatures below 550 °C (Fig. 2). However, heating of chlorite at temperatures greater than 550 °C may rearrange its structure, resulting in an intensity increase and shift in the (001) spacing to ~13.8 Å and a decrease in the intensity of the (002) spacing (Brown and Brindley, 1980). Patterns with minor heating-induced shifts in the (001) and (002) spacings were identified as chlorite in this study. Celadonite was recognized optically in nine samples and was identified by the 10-Å (001) spacing, which remains unaffected by glycerol solvation or heating at 550 °C.

The *b* crystallographic dimension of phyllosilicates is dependent on the number and type of octahedral cations and is routinely used to classify smectite (Brown and Brindley, 1980). In this study, broad (060) spacings of both dioctahedral and trioctahedral phyllosilicates were recognized. Determining the type of smectite phase based on the (060) spacings has proved inconclusive because of the admixture of phases and probable peak interference.

Randomly interlayered chlorite/smectite

Fourteen of the samples show a Mg-saturated 14-Å spacing that shifts to between 15 and 16.5 Å with glycerol solvation. The 7-Å (002) spacing broadens to the low-2θ side with glycerol solvation. Saturation with KCl results in the collapse of the (001) spacing to between 13 and 14 Å. The (001) spacing collapses further with heating at 550 °C to a broad spacing that is most intense between 12.9 and 13.8 Å and tails off to the high 2θ side (Fig. 3). A 30–33-Å superlattice spacing is not evident in these patterns, indicating that the phase is not an ordered interstratification.

The identifications made in this study are primarily based on the XRD patterns, specifically the position of the spacings after saturation with glycerol and KCl, and heat treatment. The fact that the interlayered phase expands significantly with Mg saturation and glycerol solvation

indicates that the expandable clay in these samples is not vermiculite (Walker, 1957, 1958). Because of the presence of chlorite and smectite in all but one of the samples containing the mixed-layered phase, it seems probable that the mixed-layered phase is randomly interlayered chlorite/smectite instead of chlorite/swelling chlorite. Without further study, the identification of the expandable clay as a smectite still does not preclude the possibility that it is instead another species—such as expandable chlorite.

In past studies, samples with similar XRD patterns have been identified as expandable chlorite (e.g., April, 1981; Sucheki et al., 1977), which is generally considered to be a chlorite with an incomplete brucite layer allowing for expansion upon glycerol solvation. The spacing produced, between 14 and 18 Å, is not unique. Randomly interlayered smectite/chlorite also shows (001) spacings between 14 and 18 Å with glycerol solvation.

Regularly interlayered chlorite/smectite

Regularly interlayered chlorite/smectite is typically called "corrensite," a mineral originally defined as regularly interlayered chlorite/swelling chlorite (Lippmann, 1954). However, it has subsequently been used as a name for all species of 1:1 interstratification of chlorite and an "expandable clay layer," the latter being either smectite, vermiculite, or swelling chlorite (Hauff, 1981). To avoid ambiguity we prefer to refer to this phase as "regularly interlayered chlorite/expandable clay" and refer to the expandable phase by its specific name.

Regularly interlayered chlorite/smectite was recognized by its characteristic superlattice spacing, which records the alternation of chlorite (001) 14-Å and smectite (001) 14-Å spacings in the air-dried state. The superlattice spacings identified in this study are commonly ~30 Å in the air-dried patterns and ~32.5 Å with glycerol solvation (Fig. 4). The (001) superlattice spacing was not observed after heating, but the (002) spacing at 12.2–12.6 Å would correspond to an (001) spacing of ~25 Å. The superlattice spacing is weak, possibly indicating a poorly ordered phase with additional randomly interstratified layers (April, 1981). In the Point Sal samples, smectite and chlorite are commonly recognized in addition to the regularly interlayered phase. Reported values for the superlattice spacing of regularly interlayered chlorite/smectite vary from 28 to 30 Å in the air-dried state and from 30 to 33 Å with glycerol solvation (Hauff, 1981).

Petrographic description of phyllosilicate occurrence

The samples from the volcanic units are pervasively altered and contain abundant clay minerals. The phyllosilicates fill fractures and vesicles and are present as alteration products of primary phases.

1A lavas

The common clay mineral of the 1A lavas is randomly interlayered chlorite/smectite. Minor smectite and chlorite are present (Tables 1A and 1B). Clay minerals of the 1A lavas are commonly pleochroic dark green to pale green and have first-order to upper second-order and rarely anomalous blue interference colors. Three of the 1A samples contain randomly interlayered chlorite/smectite characterized by strong pleochroism from dark bluish-green to yellow. Clay minerals that fill pore space are typically zoned from fine-grained material along the edges to coarse-grained phyllosilicates in the center (Fig. 5A). Most of the glassy groundmass of the samples is recrystallized to fine-grained phyllosilicates.

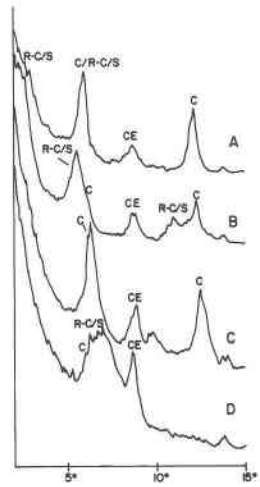

Fig. 4. X-ray pattern of regularly interlayered chlorite/smectite (R-C/S) from sample 1A-13. This sample also contains discrete chlorite (C) and celadonite (CE). (A) Mg saturated, (B) glycerol solvated, (C) KCl saturated, (D) heated at 550 °C.

Alteration of primary minerals and groundmass in the 1A lavas is pervasive and does not appear to be controlled by, or limited to, veins. Clay minerals form pseudomorphs after olivine, whereas clinopyroxene appears as predominantly fresh phenocrysts with minor alteration along fractures. Inclusions of phyllosilicates are found throughout albitized plagioclase phenocrysts (Fig. 5B); these may replace primary melt inclusions. Microphenocrysts have fewer phyllosilicate inclusions.

Celadonite is recognized in 1A lavas by its distinctive apple-green color. This phase is present as a replacement of interstitial glass and as a vesicle-filling phase. The temporal relationship between celadonite and the other phyllosilicate phases is not clear because celadonite is not observed to crosscut or fill vesicles containing other clay minerals.

Other secondary phases in the 1A lavas include albitized plagioclase, analcime, laumontite, prehnite, pumpellyite, carbonate, and quartz. The most common secondary-mineral assemblage in 1A samples is carbonate + mixed-layered chlorite/smectite + albitized plagioclase ± smectite ± minor chlorite. Carbonate is prevalent throughout the 1A lavas and is commonly found in veins. Quartz is present in the groundmass and amygdules of some of the samples, and, where present, it usually forms

TABLE 1A. Groundmass secondary-mineral assemblages of Point Sal volcanic and dike rocks

	SM	C/S	R-C/S	CH	CE	PU	EP	ACT	ALB	QTZ	CC
1A-35		X								X	
L2035	X	X		X	X				X		X
L2036	X		X		X				X	X	
1A-21	X	X		X						X	
1A-18		X								X	
1A-14	X	X		X	X				X	X	
1A-13	X		X	X					X		
1A-32	X	X		X					X		
1A-26	X	X		X					X		X
1A-25		X		X							
1A-15	X	X		X	X				X		
1A-30	X	X		X					X		
1B-60	X	X		X	X				X		
1B-42			X	X	X				X		
1B-55		X	X	X					X	X	
1B-56	X	X		X		X			X	X	
L1839			?	X					X	X	
1B-47	X	?		X					X	X	
L18B41		X		X					X		
L18B42				X					X		
1B-30			X	X					X		
1B-33	X			X							
1B-21				X					X		
1B-23				X					X	X	
1B-8				X					X		
L1746				X			X	X	X		
L1326				X			X	X			
DC-14				X			X		X		

Note: SM = smectite; C/S = randomly interlayered chlorite/smectite; R-C/S = regularly interlayered chlorite/smectite; CH = chlorite; CE = celadonite; PU = pumpellyite; EP = epidote; ACT = actinolite; ALB = albitized plagioclase; QTZ = quartz; CC = calcite.

very fine grained polycrystalline aggregates. Vesicles filled with phyllosilicates are commonly crosscut by zeolite- and/or carbonate-filled veins (Fig. 5C). Phyllosilicate-rimmed amygdules are filled in the center by carbonate. Veins filled with zeolites, either analcime or laumontite, crosscut or are cut by carbonate-filled veins. In some samples, zeolites are intergrown with carbonate, whereas in others, zeolites appear to be the first mineral to have crystallized from vein walls. Locally, prehnite grows outward from the walls of some of the veins containing analcime and laumontite (Fig. 5D).

1B lavas

The phyllosilicates of the 1B lavas are chlorite, randomly interlayered chlorite/smectite, and subordinate amounts of smectite and regularly interlayered chlorite/smectite. The clay minerals commonly have first-order and anomalous blue interference colors and are pale green in color with little or no pleochroism.

Phyllosilicates in the 1B lavas are common as replacements of interstitial glass in the groundmass, as major constituents of amygdaloidal assemblages, and as alteration of primary minerals. Vesicles are lined or completely filled by clay minerals. Clay minerals grade from fine-grained into more coarsely crystalline and platy forms that radiate outward from vesicle walls. Clinopyroxene is altered to clay minerals along fractures, but is otherwise fresh. Albitized plagioclase phenocrysts do not contain abundant phyllosilicate inclusions as in the 1A samples; instead, replacement is confined to fractures and the interstitial glass between plagioclase laths.

Calc-silicate and other authigenic phases include albitized plagioclase, pumpellyite, prehnite, epidote, garnet, actinolite, quartz, and carbonate. Common mineral assemblages for samples of the 1B lavas include pumpellyite + chlorite + albitized plagioclase ± mixed-layered chlorite/smectite ± minor smectite; pumpellyite + chlorite + quartz + albitized plagioclase ± carbonate ± mixed-layered chlorite/smectite; epidote + quartz + albite + chlorite ± carbonate. Andraditic garnet is intergrown with epidote in the rims of some amygdules filled with calcite and chlorite (Fig. 5E) and quartz. Quartz is more common in the 1B lavas than in the 1A lavas and is most often present as fillings of vesicles lined with phyllosilicates and calc-silicate minerals. It commonly forms idioblastic to subidioblastic crystals in contrast to the fine-grained aggregates present in the 1A lavas. Carbonate is less prevalent in the 1B lavas, although it is common in veins and is locally present in the center of amygdules. Clay minerals line amygdules and grade outward into or surround pumpellyite with quartz and/or carbonate in the interior (Fig. 5F). The color and birefringence of phyllosilicates intergrown with pumpellyite are similar to that of phyllosilicates replacing the groundmass and phenocrysts of 1A samples, suggesting one stage of pervasive clay-mineral recrystallization. Epidote is intergrown with

TABLE 1B. Amygdaloidal mineral assemblages in Point Sal volcanic rocks

	C/S	CH	CE	AN	LA	PR	PU	EP	GT	QTZ	CC
1A-35-a	X									X	
-b										X	X
L2036											X
1A-21	X										X
1A-18-a	X										
-b	X										X
-c											X
1A-14	X									X	
1A-13-a	X										X
-b											X
1A-32-a	X										X
-b			X								
1A-26											X
1A-25-a	X										
-b				X							
-c					X						
1A-15											X
1A-30-a											X
-b				X							
-c				X							X
1B-60				X							
1B-55-a						X				X	
-b										X	X
-c										X	
1B-56-a		X					X			X	
-b							X	X		X	
L1839		X								X	X
1B-47-a									X	X	
-b										X	X
-c								X		X	X
L18B41-a							X			X	
-b		X					X				
-c		X					X			X	
-d		X					X			X	X
-e							X			X	X
1B-23-a		X						X	X		X
-b								X		X	
-c										X	
-d		X						X			X

Note: For abbreviations, see Table 1A except that here C/S = randomly and regularly interlayered chlorite/smectite, AN = analcime, LA = laumontite, PR = prehnite, and GT = garnet.

idioblastic to subidioblastic quartz crystals and locally appears as a pseudomorph after pumpellyite in the form of elongate blades oriented in radial aggregates. Prehnite is rare in the 1B lavas; when present, it occurs in the center of amygdules lined with quartz. Hematite occurs locally in some strongly epidotized brecciated lavas.

Late-stage carbonate veins crosscut veins and vesicles containing quartz, epidote, or pumpellyite. Quartz and carbonate commonly contain inclusions of phyllosilicates, which suggests a late stage of phyllosilicate alteration. Celadonite is also present as late-stage vesicle fillings in the upper 1B lavas.

Dike and sill complex

Phyllosilicates in the dike and sill complex are predominantly chlorite. Chlorite replaces the fine-grained mesostasis in samples of the dike and sill complex. Chlorite is identified by the typical pale green color and pleochroism and anomalous interference colors.

Other metamorphic phases include epidote, actinolite, albitized plagioclase, and quartz. Common mineral assemblages of the dike and sill complex are epidote + actinolite + chlorite + albitized plagioclase + quartz; epidote + chlorite + quartz. Actinolite needles are commonly intergrown with chlorite and epidote. Plagioclase is only slightly altered to chlorite along cracks. Epidote occurs in patches in the groundmass of dike and sill rocks and also in epidositic dikes with quartz and chlorite. Pyrite is present in some epidosite dikes.

PHYLLOSILICATE ZONATION VS. STRATIGRAPHY

Tables 1A and 1B list the minerals identified in each sample studied and the phyllosilicates that were recognized by X-ray diffractometry. As mentioned above, the dominant phyllosilicates in the 1A lavas are randomly interlayered chlorite/smectite and smectite. Only minor amounts of chlorite are present in samples from the upper lavas. Randomly interlayered chlorite/smectite and smectite are less common in the 1B lavas. These two phyllosilicate phases diminish in occurrence, and chlorite becomes the dominant sheet silicate with increasing depth. Chlorite becomes the most abundant phase in the lower 1B section and the dike and sill complex. Smectite found

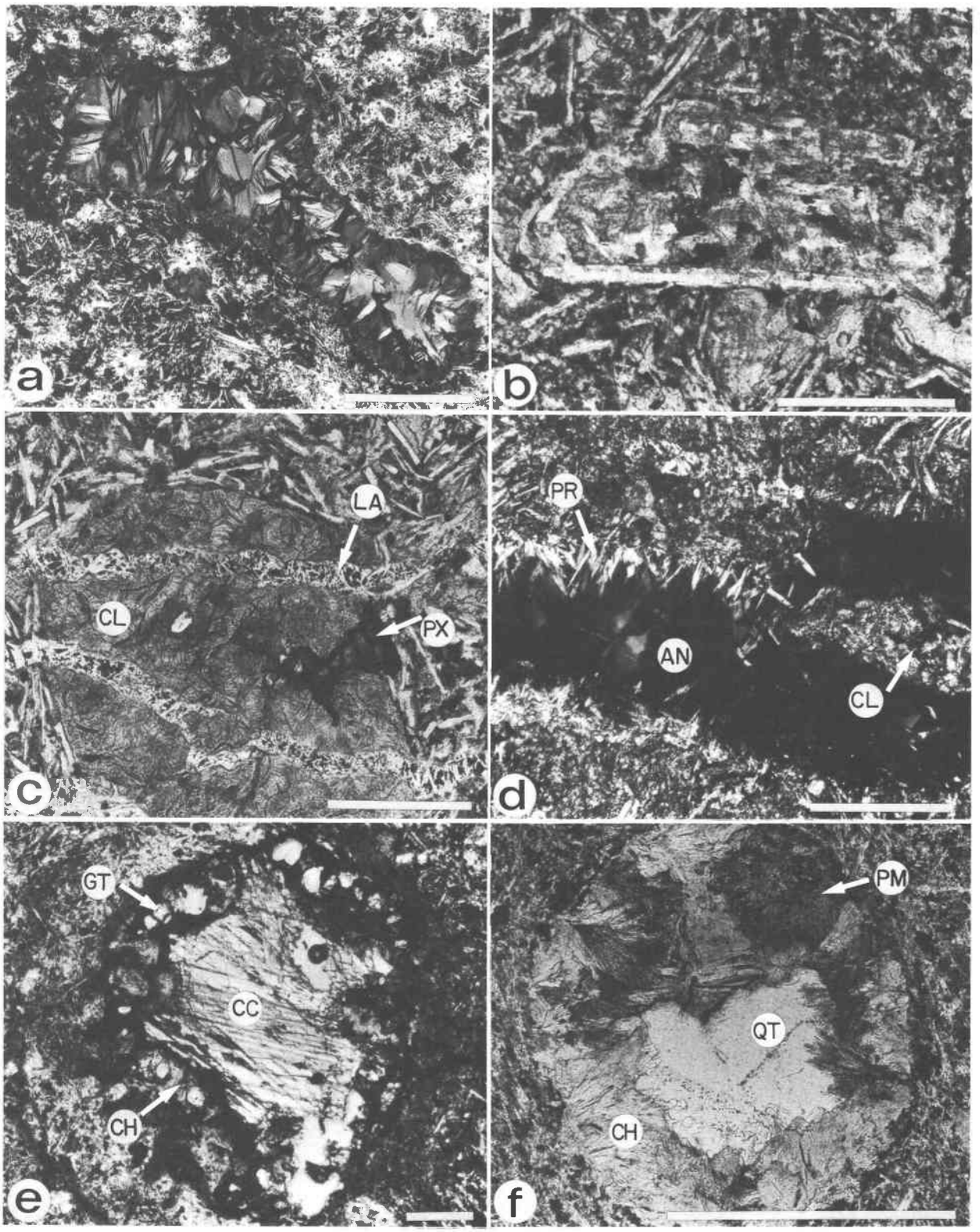

Fig. 5. Photomicrographs of mafic phyllosilicates and related minerals from Point Sal volcanic rocks (scale bars = 0.1 mm). (A) Fine-grained, randomly interlayered chlorite/smectite grading into coarser-grained forms in the center of the amygdule (sample 1A-25). Photomicrograph taken with plane-polarized light. (B) Albitized plagioclase with inclusions of randomly interlayered chlorite/smectite alteration (sample 1A-8). Photomicrograph taken with plane-polarized light. (C) Pseudomorph after pyroxene grain.

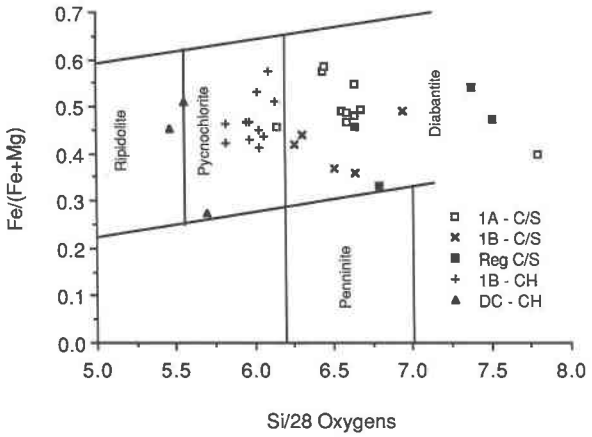

Fig. 6. Fe/(Fe + Mg) vs. Si compositional variations of phyllosilicates in the Point Sal remnant. Cations were calculated on the basis of 28 oxygens from average analyses (Bettison, 1986). Modified after Hey (1954). 1A = upper lavas; 1B = lower lavas; DC = dike and sill complex; C/S = randomly interlayered chlorite/smectite; Reg C/S = regularly interlayered chlorite/smectite; CH = chlorite.

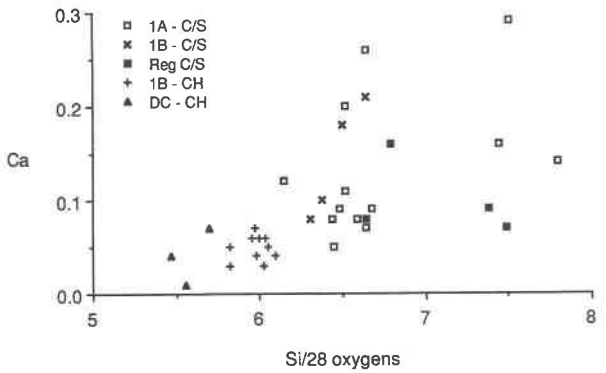

Fig. 7. Ca vs. Si for average analyses of interlayered chlorite/smectite and chlorite in the Point Sal remnant. Structural formulae calculated on the basis of 28 oxygens. C/S = randomly interlayered chlorite/smectite; Reg C/S = regularly interlayered chlorite/smectite; CH = chlorite.

in minor quantities in the latter section is probably a much later phase, as indicated by textural relations.

Chemical analyses

In order to characterize the phyllosilicates, compositional data were obtained through energy-dispersive electron-microprobe analysis. Because of the fine-grained and porous nature of many of the phyllosilicate aggregates, anhydrous oxide totals from microprobe analyses varied significantly (84–90 wt%). Therefore, the representative analyses presented in Table 2 include only cationic proportions. Complete oxide analyses, including those for celadonite, can be found in Bettison (1986).

Compositions of chlorite fall mostly in the pycnochlorite field of Hey's (1954) chlorite classification (Fig. 6). Randomly interlayered chlorite/smectite compositions fall within the diabantite field. Silica decreases with increasing pseudostratigraphic depth and with the transition from smectite to chlorite. Randomly interlayered chlorite/smectite of the 1A lavas have Si contents that fall predominantly in the range of 6.15–6.70 cations on the basis of 28 oxygens. Si in randomly interlayered chlorite/smectite of the 1B lavas ranges from 6.30 to 6.80 cations/28 oxygens. Chlorite from the 1B lavas has lower Si contents (5.82–6.14 cations/28 oxygens) than the mixed-layered phases, and chlorite from the dike and sill complex has the lowest Si contents (5.45–5.70). The phyllosilicates have corresponding Al contents that increase with increasing depth and with the transition to discrete chlorite in the 1B lavas and the dike and sill complex: (Al cations/28 oxygens: 1A, 2.54–3.61; 1B, 3.48–4.58; DC, 4.40–4.91). An increase in Fe/Mg with increasing metamorphic grade is not apparent in the Point Sal phyllosilicates, though this increase has been documented in other ophiolites (e.g., the Del Puerto remnant by Evarts and Schiffman, 1983).

Interlayered chlorite/smectite has more variable composition than discrete chlorite (Table 2). The interstratified species contain predominantly Si (7.80–6.15 cations/28 oxygens), Al (4.13–2.50), Fe (6.14–3.11), and Mg (5.96–4.34), with minor Mn (0.17–0.05), K (0.55–0), and Ca (0.26–0). Chlorite can accommodate only a minor amount of Ca in its structure. Therefore, analyses with Ca contents of more than 0.10 cation/28 oxygens indicate the presence of a smectite component as confirmed by X-ray diffraction. Figure 7 shows that the Ca contents of the phyllosilicates from the volcanic and dike units range from 0 to 0.30 cations per 28 oxygens; the Ca content decreases with increasing pseudostratigraphic depth and metamorphic grade. Phyllosilicates of the 1A lavas contain the most Ca in interlayer sites. The 1A samples contain the largest smectite component and have more sites available to Ca. The least Ca is found in the chlorite from the 1B lavas and the dike and sill complex.

←

Composed of randomly interlayered chlorite/smectite (CL) with intergrown fine-grained pumpellyite, crosscut by veins containing laumontite (LA) and prehnite (sample 1A-8). Photomicrograph taken with plane-polarized light. PX = relict pyroxene. (D) Analcime (AN) + prehnite (PR) vein (sample 1A-8). Photomicrograph taken with cross-polarized light. CL = mixed-layered chlorite/smectite. (E) Andraditic garnet (GT) intergrown with chlorite (CH) and calcite (CC) in amygdules of sample 1B-23. Photomicrograph taken with plane-polarized light. (F) Amygdaloidal pumpellyite (PM) intergrown with chlorite (CH) and quartz (QT) in sample L18B41. Photomicrograph taken with plane-polarized light.

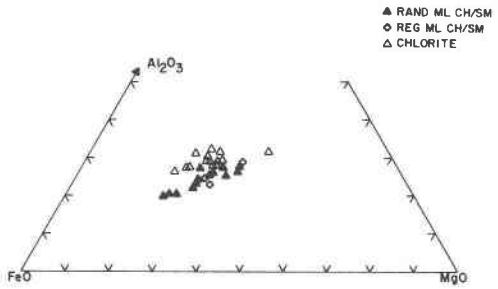

Fig. 8. Al_2O_3-FeO-MgO compositions of Point Sal mafic phyllosilicates (normalized weight percent of average analyses from Table 2).

Chemical variations of the interlayered chlorite/smectite and chlorite are represented on an Al_2O_3-MgO-FeO compositional plot depicting averaged microprobe analyses (Fig. 8). The Fe/Mg ratio in interstratified phases varies significantly, but Al contents are consistently lower than in chlorite. However, some of the interlayered species do have compositions very similar to those of the discrete chlorite plotted. It is important to note that regularly and randomly interlayered chlorite/smectite do not have Al_2O_3-MgO-FeO ratios that are significantly different, and they cannot be unambiguously differentiated using this ternary diagram (Fig. 8).

Ideally, structural recalculation of a relatively pure sample of regularly interlayered chlorite/smectite on the basis of (28 + 22)/2 oxygens should determine the number of octahedral sites in both layers. The assumption made is that this regularly interlayered phase is indeed 1:1 chlorite/smectite, and therefore, the structural formula corresponds to ½ unit cell chlorite + ½ unit cell smectite. The total octahedral cations should be 9 if both the smectite and chlorite are trioctahedral, or 7.5 if one of the layers is dioctahedral. For example, the total of octahedral occupancy in sample L2036 is 9.57, which is close to the ideal 9. Thus, both the smectite and chlorite layers are nearly trioctahedral. Although no analyses of pure smectite were obtained, the Fe-rich aggregate composition of the mixed-layered phases suggests that the smectite component is most likely saponite.

The chlorite/smectite analyses can be recast into unit-cell contents with variable oxygen if both the minerals are assumed to be trioctahedral. If the analyzed phase lies between pure saponite and pure chlorite, the composition will be expressed by $(K,Na,Ca_{0.5})_{z-y}{}^{VI}[(Mg,Fe,Mn)_{6-y}Al_y]\text{-}{}^{IV}[Si_{8-z}Al_z]O_{20}(OH)_4 \cdot x[(Mg,Fe)_6(OH)_{12}]$. Values for x, y, and z can be obtained from the above formula by first calculating a proportioning factor (f). The factor can be determined for two different cases: (1) if $z > y$, $f = 16/[Al + 2Si + 2Ca + K]$ and (2) if $z < y$, $f = 16/[Al + 2Si - 2Ca - K]$ (W. Wise, pers. comm., 1987). Judging from

TABLE 2. Structural formulae of average phyllosilicate compositions based on 28 oxygens

Sample	Phase*	K	Ca	Total	Mn	Mg	Fe	^{VI}Al	Total	Si	^{IV}Al	Total	Range in Si	Range in Fe/Mg	Oxide total
1A-35	C/S	0.01	0.05	0.06	0.08	4.34	6.14	1.44	12.01	6.45	1.55	8.00	6.40–6.51	0.57–0.61	87.83
L2035	C/S	0.50	0.14	0.64	0.17	4.66	3.11	2.51	10.45	7.80	0.20	8.00	7.80	0.40	88.10
L2036	R-C/S	0.55	0.07	0.62	0.08	4.35	3.94	2.35	10.72	7.49	0.51	8.00	7.32–7.65	0.47–0.48	85.10
1A-21	C/S	0.40	0.11	0.15	0.10	5.00	4.77	1.81	11.68	6.52	1.48	8.00	6.45–6.65	0.47–0.51	84.28
1A-18	C/S	0.01	0.08	0.09	0.09	4.40	5.95	1.49	11.84	6.44	1.56	8.00	6.38–6.47	0.55–0.59	88.88
1A-14	C/S	0.02	0.07	0.09	0.09	4.56	5.50	1.63	11.78	6.64	1.36	8.00	6.46–6.82	0.50–0.57	87.83
1A-13	R-C/S	0.03	0.08	0.11	0.06	5.37	4.48	1.76	11.67	6.64	1.36	8.00	6.50–6.81	0.43–0.47	86.77
1A-32	C/S	0.04	0.09	0.13	0.14	4.94	4.83	1.75	11.66	6.68	1.32	8.00	6.51–6.81	0.48–0.50	88.14
1A-26	C/S	0.05	0.26	0.31	0.13	4.60	4.27	2.25	11.25	6.64	1.36	8.00	6.45–6.80	0.46–0.51	89.58
1A-25	C/S	0.02	0.12	0.14	0.11	5.45	4.58	1.76	11.90	6.15	1.85	8.00	6.13–6.27	0.44–0.47	87.61
1A-15	C/S	0.05	0.08	0.13	0.05	5.11	4.44	1.98	11.58	6.59	1.41	8.00	6.44–6.86	0.45–0.48	88.31
1A-30	C/S	0.04	0.08	0.12	0.10	4.99	4.81	1.84	11.74	6.47	1.53	8.00	6.43–6.52	0.49–0.50	85.61
1B-60	C/S	0.00	0.18	0.18	0.09	5.96	3.51	2.00	11.56	6.50	1.50	8.00	6.34–6.67	0.36–0.38	89.51
1B-42	R-C/S	0.03	0.16	0.19	0.19	5.85	2.97	2.29	11.30	6.79	1.21	8.00	6.79	0.34	83.21
1B-55A	C/S	0.04	0.08	0.12	0.09	5.38	4.30	1.98	11.75	6.31	1.69	8.00	6.31	0.44	88.09
1B-55B	CH	0.02	0.06	0.08	0.09	5.51	4.20	2.08	11.88	6.00	2.00	8.00	5.95–6.04	0.42–0.44	88.06
1B-56A	C/S	0.25	0.00	0.25	0.05	4.67	4.57	2.07	11.36	6.95	1.05	8.00	6.95	0.49	87.11
1B-56B	CH	0.02	0.00	0.02	0.05	5.02	4.41	2.35	11.83	5.97	2.03	8.00	5.95–5.99	0.46–0.47	88.17
L1839	CH	0.02	0.06	0.08	0.11	5.03	4.37	2.29	11.80	5.95	2.05	8.00	5.84–6.01	0.45–0.48	87.82
1B-47	CH	0.00	0.05	0.05	0.09	4.58	5.01	2.16	11.84	6.05	1.95	8.00	5.97–6.10	0.49–0.54	88.27
L18B41	CH	0.00	0.05	0.05	0.09	5.19	4.46	2.20	11.94	5.82	2.18	8.00	5.76–5.88	0.45–0.47	87.66
L18B42	CH	0.00	0.04	0.04	0.09	4.08	5.52	2.15	11.84	6.09	1.91	8.00	5.95–6.17	0.54–0.59	87.21
1B-30A	R-C/S	0.07	0.09	0.16	0.07	3.12	3.66	3.51	10.36	7.38	0.62	8.00	7.38	0.54	88.11
1B-30B	CH	0.01	0.03	0.04	0.09	4.47	5.09	2.17	11.82	6.02	1.98	8.00	5.91–6.13	0.52–0.55	88.71
1B-33A	C/S	0.04	0.10	0.14	0.08	5.56	3.83	2.11	11.58	6.38	1.62	8.00	6.22–6.56	0.38–0.43	88.73
1B-33B	CH	0.02	0.06	0.08	0.08	5.28	4.27	2.15	11.78	6.03	1.97	8.00	6.02–6.05	0.44–0.45	89.88
1B-21	CH	0.02	0.04	0.06	0.08	5.60	3.94	2.21	11.83	5.98	2.02	8.00	5.78–6.11	0.40–0.42	90.10
1B-23	CH	0.03	0.07	0.10	0.08	5.48	4.12	2.16	11.84	5.97	2.03	8.00	5.82–6.10	0.41–0.45	88.65
1B-8	CH	0.02	0.03	0.05	0.08	5.31	3.98	2.45	11.82	5.82	2.18	8.00	5.57–6.07	0.41–0.43	87.95
L1746	CH	0.00	0.01	0.01	0.05	4.69	4.92	2.36	12.02	5.56	2.44	8.00	5.35–5.77	0.49–0.53	89.73
L1326	CH	0.00	0.04	0.04	0.08	5.24	4.35	2.38	12.05	5.47	2.53	8.00	5.44–5.52	0.43–0.48	88.46
DC-14	CH	0.00	0.07	0.07	0.06	7.17	2.69	2.10	12.02	5.70	2.30	8.00	5.63–5.98	0.27–0.29	87.75

* For abbreviations, see Table 1.

analyses presented in Table 2, it appears that the latter case is most likely. Recalculated analyses of representative samples of interlayered chlorite/smectite and chlorite are listed in Table 3. Structural-formulae recalculation of interlayered phases on this basis represents a possible technique by which to evaluate the proportions of saponite and chlorite. For analyses representing pure chlorite, x will approach one and the exchangeable cations will be near zero. Pure saponite will be represented by analyses in which x is zero. Interlayered phases with 1:1 proportions of chlorite and saponite should have x near 0.5.

The most common method for determining the mole fraction of chlorite present in the interlayered phase is based on the position of the combined (001) peaks of chlorite and smectite on X-ray diffractograms. The mole fractions of chlorite determined using the method developed by Hower (1981) are listed in Table 3 for comparison with the results of the structural-formulae recalculation method. The error in estimating the mole fraction of chlorite is approximately ±10% of the true value because of the error in resolution of ±0.2° 2θ in the peak position from the X-ray diffractograms. In addition, error may result from the variation in thickness of the ethylene glycol complex within the saponite layers. Hower's method assumes expansion of pure saponite to 16.9 Å in ethylene glycol, though the actual thickness of these layers may range from 16.6 to 17.2 Å (J. Środoń, 1980). In most of the analyses presented in Table 3, the mole fraction of chlorite interlayers estimated from X-ray diffractograms is bracketed by that determined from the two possible methods of structural-formulae recalculation. Thus, it appears that microprobe analyses of interlayered trioctahedral smectite/chlorite minerals can be recalculated to give useful estimates of the proportions of the interlayer end members.

TABLE 3. Phyllosilicate analyses recalculated to estimate relative proportions of chlorite interlayers

	L2035		L2036		1A-13		1A-30		1B-60		1B-42		1B-30		L1326	
	$z > y$	$z < y$	$z > y$	$z < y$	$z > y$	$z < y$	$z > y$	$z < y$	$z > y$	$z < y$	$z > y$	$z < y$	$z > y$	$z < y$	$z > y$	$z < y$
Si	6.54	7.12	6.46	7.00	6.40	6.55	6.27	6.42	6.17	6.44	6.23	6.49	5.92	5.97	5.49	5.52
Al_z	1.46	0.88	1.54	1.00	1.60	1.45	1.73	1.58	1.83	1.56	1.77	1.51	2.08	2.03	2.51	1.48
Al_y	0.81	1.59	0.93	1.67	1.41	1.63	1.53	1.77	1.49	1.91	1.45	1.84	2.00	2.09	2.43	3.48
Mg	3.91	4.25	3.75	4.06	5.18	5.30	4.83	4.95	5.66	5.91	5.37	5.59	4.40	4.43	5.26	5.29
Fe	2.61	2.84	3.40	3.68	4.32	4.42	4.66	4.78	3.33	3.48	2.73	2.84	5.01	5.05	4.37	4.39
Mn	0.14	0.15	0.07	0.07	0.06	0.06	0.10	0.10	0.08	0.09	0.17	0.18	0.09	0.09	0.08	0.08
Ca	0.12	0.13	0.06	0.06	0.08	0.08	0.08	0.08	0.17	0.18	0.15	0.15	0.03	0.03	0.04	0.04
K	0.42	0.46	0.47	0.51	0.03	0.03	0.04	0.04	0.00	0.00	0.03	0.03	0.01	0.01	0.00	0.00
x	0.24	0.47	0.36	0.58	0.83	0.90	0.85	0.93	0.76	0.90	0.62	0.74	0.92	0.94	1.02	1.21
x^*	0.40		0.60		0.70		0.90		0.80		0.70		1.00		1.00	

Note: Recalculation of formula proportions (presented in Table 2) using method based on layer charge balance and Al partitioning (see text); z = Al in tetrahedral sites; y = Al in octahedral sites; x = proportion of brucite layers = mole fraction chlorite in interlayered phase (see text).

* Estimation of the mole fraction chlorite layers from X-ray diffractograms using the method of Hower (1981); the estimations are considered accurate to ±10% of the stated values (see text).

Discussion

Compositional variations of mafic phyllosilicates

Although the compositional variations of mafic phyllosilicates from low-grade metabasaltic rocks have been extensively characterized (Bass, 1976; Robinson et al., 1977; Scheidegger and Stakes, 1980), there have been no attempts to correlate compositional variations with the structures of these phases. This is because detailed and systematic X-ray diffraction studies of these minerals in combination with electron-microprobe analyses are rare. Mafic phyllosilicate compositions reflect structural differences that may be strongly temperature dependent. Is it possible to differentiate low-grade mafic phyllosilicates by compositional information alone? In this discussion, we compare the major- and minor-element contents of mafic phyllosilicates from ophiolites and other hydrothermally altered rocks (e.g., oceanic basalts and active geothermal systems) in order to evaluate the systematics of their compositional variations. Our discussion is limited to those data bases that include both compositional and X-ray diffraction analysis. Classification of phyllosilicates is

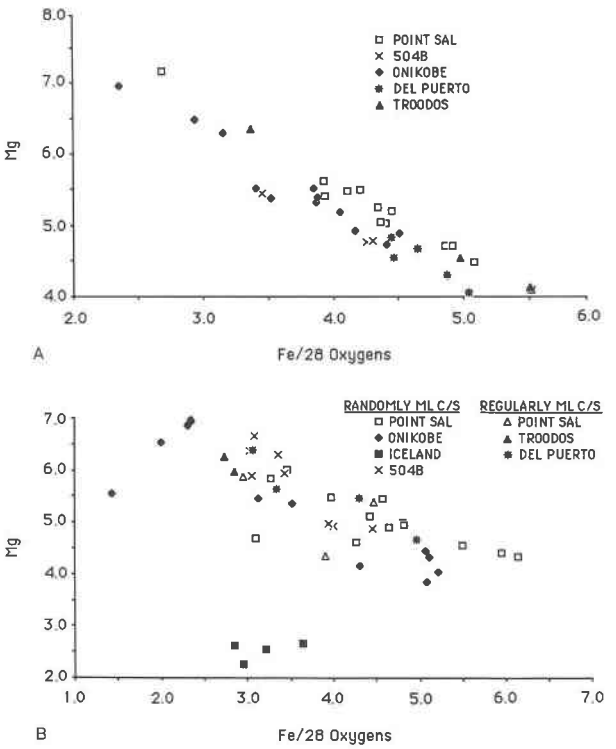

Fig. 9. Mg vs. Fe for (A) chlorite and (B) interlayered chlorite/smectite from Point Sal (this study), Del Puerto (Evarts and Schiffman, 1983), Onikobe geothermal field (Seki et al., 1983), Icelandic geothermal fields (Kristmannsdóttir, 1975), DSDP Hole 504B (Alt et al., 1985), and Troodos (Schiffman and Smith, 1988). ML C/S = mixed-layered chlorite/smectite.

commonly attempted using only one of these techniques. Chlorite in particular is often identified solely on the basis of compositional analysis without the benefit of X-ray diffraction analysis to confirm its existence.

Figure 9A indicates that the Fe and Mg contents of discrete chlorite exhibit nearly one-to-one substitution. Data from Point Sal, Del Puerto, 504B, Troodos, and Onikobe indicate that the total (Fe + Mg) contents of chlorite are generally from 9.0 to 9.5 octahedral cations per 28 oxygens. The variation in Fe and Mg contents, particularly within any one of the localities represented, suggests that local altered bulk-rock or hydrothermal-fluid composition controls the concentration of each of these elements in the phyllosilicate.

Figure 9B indicates that the total (Fe + Mg) is more variable in mixed layered chlorite/smectite. The total octahedral cation content is lower in smectite than in chlorite when computed on the basis of 28 oxygens, and variation in the amount of interstratified smectite would cause marked variations in octahedral occupancy.

The relationship of Ca to Si in mixed-layered phyllosilicates from Onikobe, 504B, and Del Puerto is similar to that at Point Sal (Fig. 10). The greater the amount of interlayered smectite, and presumably silica content, the greater the amount of Ca that the phase will contain. This

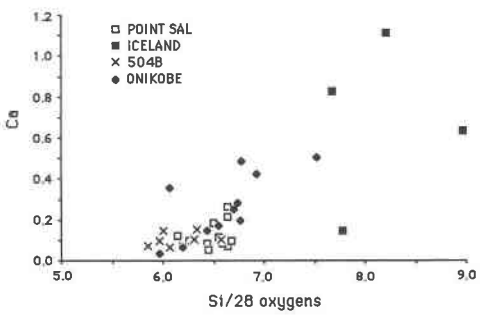

Fig. 10. Ca vs. Si variation diagram for interlayered chlorite/smectite. Structural formulae calculated on the basis of 28 oxygens. (See caption of Fig. 9 for data sources.)

appears to be directly related to temperature as it is clear that, with increasing depth, the silica content decreases as chlorite predominates over the mixed-layered phases.

Although the Ca content of mixed-layered phases is directly attributable to the smectite component, it is not clear what controls the presence of Ca in chlorite. There is no correlation between the amount of Ca and the amount of Al, Fe, Si, or Mg found in chlorite (Bettison, 1986). The Ca contents of Del Puerto chlorite (0.01 cations per 28 oxygens) are lower than those from the other localities with the exception of one sample. The Ca in chlorite may suggest the presence of "islands" of smectite remaining within the structure. Perhaps the lower Ca content present in chlorite from the Del Puerto remnant suggests that this chlorite is a product of a slightly higher grade of metamorphism than is the chlorite from the Point Sal remnant.

Figure 11 compares the silica cation contents from Point Sal phyllosilicates to those from the examples of submarine hydrothermal systems discussed above. Analyses of phyllosilicates from Del Puerto and Point Sal are similar. However, the Si and Ca contents of Del Puerto chlorite are lower than are those from Point Sal volcanic rocks. Analyses by Gillis and Robinson (1985) and Schiffman and Smith (1988) of phyllosilicates from volcanic rocks of Troodos indicate higher Si content than found at Point Sal. Phyllosilicate zonation at Point Sal indicates that the transition from smectite to true chlorite occurs in the volcanic units, whereas chlorite is rarely found in the volcanic units at Troodos except beneath and adjacent to massive sulfide deposits (Schiffman and Smith, 1988). At a given depth in the volcanic member, the phyllosilicates from Troodos are generally of much lower grade than those in the Coast Range ophiolite remnants (Fig. 11). The phyllosilicate silica contents from the Onikobe geothermal field are also similar to those from Point Sal.

The compositional transition from mixed-layered chlorite/smectite to chlorite appears to occur within the range of 6.25 to 5.95 cations (per 28 oxygens) for hydrothermally altered volcanic rocks recrystallized under low-pressure and low-temperature conditions. This apparently holds true for all of the fields plotted in Figure 11, with the exception of DSDP 417A. Given this, some guidance can be applied to those samples simply identified by com-

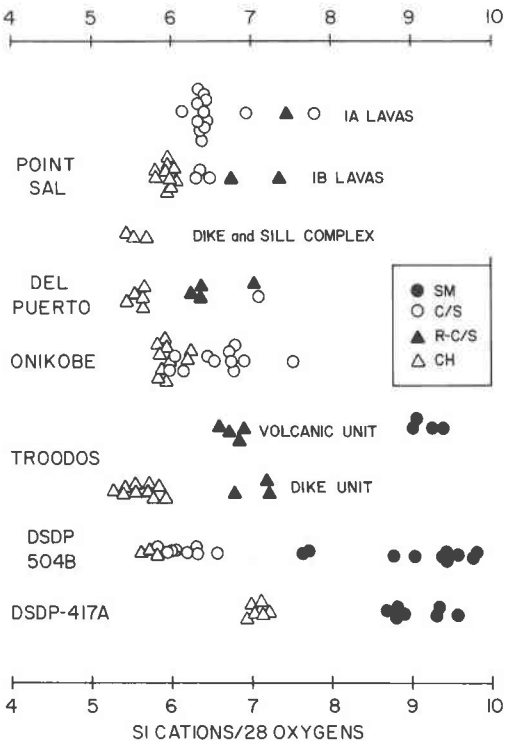

Fig. 11. Comparison of Si cations/28 oxygens of phyllosilicates from Point Sal to those from other low-pressure and low-temperature, hydrothermally altered volcanic rocks (refer to caption of Fig. 9 for data sources; DSDP-417A data from Pritchard, 1980). SM = smectite, C/S = randomly interlayered chlorite/smectite; R-C/S = regularly interlayered chlorite/smectite; CH = chlorite. Note that Point Sal data are averaged analyses and others are individual data points.

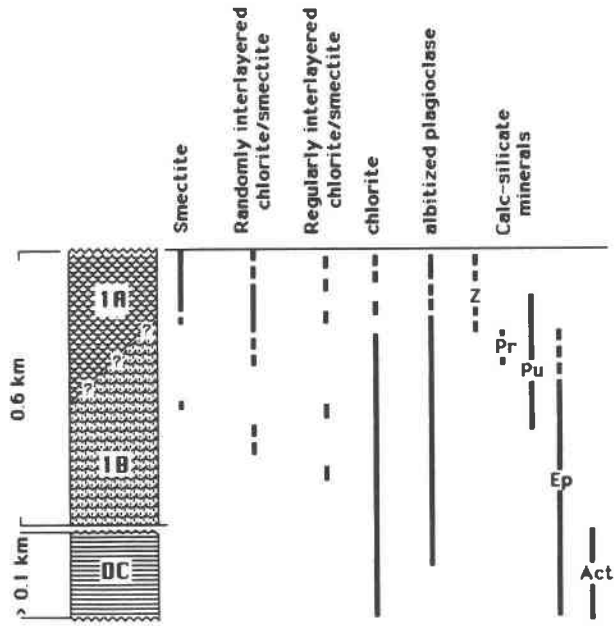

Fig. 12. Phyllosilicate and calc-silicate mineral zonations within the volcanic units and dike and sill complex of the Point Sal ophiolite. Z = zeolites (analcime and laumontite); PR = prehnite; PU = pumpellyite; EP = epidote; ACT = actinolite. Andradite garnet is locally present in 1B lavas.

positional analysis alone. For example, Pritchard (1980) has documented the occurrence of chlorite in DSDP Hole 417A and has referred to X-ray diffraction data without indicating whether glycerol solvation and/or heating of the oriented slides was performed. Si cation contents for analyses of chlorite from 417A are plotted on Figure 12. These distinctly place 417A "chlorite" within a range that would be reasonable for a mixed-layered phase. The CaO contents (0.24–1.10 wt%—Pritchard, 1980; Table 4) are also unreasonable for the chlorite structure. Re-examination of the 417A data may indicate that "chlorite" actually has a component of interlayered smectite. We suggest that any microprobe analysis of a low-temperature mafic phyllosilicate that contains greater than 6.2 cations/28 oxygens cannot be assumed to be chlorite in the absence of systematic X-ray diffraction studies.

Factors controlling phyllosilicate mineral formation in Point Sal volcanic rocks

Temperature

The lack of abundant smectite and low-temperature authigenic zeolites (e.g., clinoptilolite, phillipsite) within the volcanic units at Point Sal suggests that the grade of metamorphism is higher than that in oceanic basalts and the Troodos ophiolite (Alt et al., 1986; Schiffman and Smith, 1988). The secondary-mineral zonation at Point Sal is very similar to that of the Del Puerto remnant and active geothermal fields (Schiffman et al., 1984; Bird et al., 1984).

The occurrence of laumontite, analcime, and mixed-layered clays in the 1A lavas suggests that the temperature at which the upper volcanic unit was altered was approximately 125 °C (Fig. 12). The temperature maximum of analcime + quartz has been experimentally determined to be 200 °C (Thompson, 1971a; Liou, 1971); however, the upper temperature limit in natural systems would be lower (Evarts and Schiffman, 1983). Laumontite is present in geothermal fields at temperatures below 200 °C (Bird et al., 1984) and occurs with albite in burial metamorphic environments at temperatures of approximately 100 °C (Evarts and Schiffman, 1983). In addition, Kristmannsdóttir (1975, 1979) has recorded the presence of mixed-layered chlorite/smectite at temperatures less than 200 °C in Icelandic geothermal fields. Keith et al. (1984) have documented the transition from smectite to predominantly mixed-layered smectite/chlorite and discrete chlorite at approximately 150 °C at the Newberry volcano in Oregon. Evarts and Schiffman (1983) have suggested that the formation of pumpellyite from laumontite + mixed-layered phyllosilicates at Del Puerto occurs at approximately 125 °C, marking the transition from the zeolite-facies to the prehnite-pumpellyite facies. This temperature is also reasonable for the transition from the

zeolite facies to the prehnite-pumpellyite facies at Point Sal.

Kristmannsdóttir (1975, 1979) and Franzson et al. (1986) reported that the transition from mixed-layered chlorite/smectite to discrete chlorite occurs between 200 and 240 °C in the Icelandic geothermal fields. Epidote occurs in geothermal fields at temperatures greater than 200–250 °C (Bird et al., 1984). These temperatures are consistent with the temperatures mentioned for the transition to metamorphic chlorite; however, O-isotope temperatures for hydrothermal beidellite and mixed-layered chlorite/smectite from the East Pacific Rise along 21°N are in the range 290–360 °C (Haymon and Kastner, 1986). At Point Sal, pumpellyite breaks down to epidote at slightly deeper levels than the level at which mixed-layered chlorite/smectite transformed to chlorite (Fig. 12). The order of these two transitions is the same in the Del Puerto remnant (Evarts and Schiffman, 1983) where the transition from the pumpellyite facies to the epidote facies was estimated to occur at approximately 225 °C. The lack of abundant actinolite in the volcanic units indicates that temperatures did not exceed 300 °C (Ellis, 1979; Bird et al., 1984). The isolated presence of andradite garnet + epidote assemblages, which occur in geothermal fields at temperatures of approximately 300 °C, may suggest local thermal or hydrothermal fluxes within the 1B lavas

Pressure

The pressure attending hydrothermal metamorphism of Point Sal volcanic rocks may be inferred from volcanogenic features and the known stabilities of coexisting calc-silicate minerals. Many features of the volcanic units at Point Sal, such as the generally vesicular nature of the lavas and the occurrence of breccia and segregation vesicles, are similar to those described from Del Puerto (Evarts and Schiffman, 1983). The major difference between the two remnants is that pillow lavas are common in the 1B volcanic unit at Point Sal but are scarce at Del Puerto. In spite of this difference, these features suggest that the eruption of the lavas at Point Sal and Del Puerto occurred at shallow water depths (see discussion by Evarts and Schiffman, 1983). The fluid pressure at the Del Puerto basalt-seawater interface was estimated to be approximately 100 bars. Lawsonite is absent; therefore, the maximum fluid pressure is constrained by the nearly isobaric breakdown of laumontite to lawsonite at 3 kbar (Liou, 1971). Submarine hydrothermal metamorphism of volcanic and dike rocks within modern oceanic spreading centers apparently occurs at pressures not greatly exceeding 450 bars (Bischoff, 1980; Seyfried, 1987).

Water/rock ratios, fluid composition, and oxygen fugacity

The suggestion that the Point Sal remnant was recrystallized in a submarine hydrothermal system is supported by O-isotope data from the volcanic units (Schiffman et al., 1986) that indicate that rocks of the volcanic units and dike and sill complex have been moderately to strongly enriched in ^{18}O. High water/rock ratios would also tend to produce a preponderance of high-variance mineral assemblages (i.e., low number of phases), such as are observed in the Point Sal volcanic rocks (Table 1B). The pervasive style of metamorphism of the ophiolite also supports the conclusion that large volumes of water flowed through these rocks during hydrothermal metamorphism. If water/rock ratios were high, fluid chemistry would be an important factor in the resulting composition of secondary minerals.

High f_{O_2} is suggested by the high Fe_2O_3 contents of epidote, prehnite, and pumpellyite (Bettison, 1986). The localized presence of celadonite and hematite and the composition of the smectite phase (saponite) are also compatible with a relatively high oxygen fugacity.

High activities of Ca and reduced p_{CO_2} generally favor the formation of calcic zeolites and other calc-silicate minerals over the formation of clay minerals (Hay, 1978; Thompson, 1971b; Zen and Thompson, 1974). Phyllosilicates also form in the presence of Ca-rich fluids but are not destabilized at high p_{CO_2} (Zen, 1959). Apparently p_{CO_2} was relatively high during the initial alteration of Point Sal volcanic rocks. It is suggested that the phyllosilicate phases formed prior to and during the formation of calc-silicate minerals, indicating that the p_{CO_2} decreased with increase in temperature. The destabilization of interlayered chlorite/smectite with increase in temperature releases Ca into the fluid as does the albitization of calcic plagioclase. The Ca released into the system is ultimately partitioned into calc-silicate minerals such as epidote and actinolite.

The formation of regularly interlayered chlorite/smectite during the transition from smectite to chlorite may not be completely temperature dependent. Experimental studies at 2 kbar and temperatures greater than 300 °C (Velde, 1977) suggest that the occurrence of the regularly interstratified phase may be controlled by the R^{3+} component (the Al^{3+} or Fe^{3+} content of the assemblage). In addition, Velde (1977) has shown that it is possible for both chlorite and regularly interlayered chlorite/smectite to form at similar temperatures. Velde's experiments show that the regularly interlayered phase will concentrate Mg in its structure whereas chlorite will partition Fe. The fact that the lower lavas are generally Mg-enriched with respect to upper lavas (Schiffman et al., 1986) may or may not suggest that fluids altering the former had high Mg activity contributing to the formation of the regularly interstratified phases.

Conclusions

Detailed X-ray diffraction and compositional analyses of phyllosilicates from the Point Sal remnant indicate that the transition from smectite to chlorite is temperature sensitive and that the structural changes involved in this transition have correlative compositional trends. The reduction in interlayer Ca and the decrease in Si as mixed-

layered chlorite/smectite transforms to chlorite reflects the continuing destabilization of smectite layers with increasing temperature.

The transition from interlayered chlorite/smectite to chlorite roughly parallels the transition from the prehnite-pumpellyite to the prehnite-actinolite facies as defined by calc-silicate mineral assemblages (Liou et al. 1987). In low-pressure hydrothermal systems, this transition has been shown to occur at temperatures between 200 and 230 °C, correlative with the first appearance of epidote in active geothermal systems. In the Point Sal remnant, mixed-layered chlorite/smectite is the dominant phyllosilicate of the upper (1A) lavas, whereas chlorite is more abundant within the lower (1B) lavas. Within the pseudostratigraphy of the Point Sal ophiolite, this phyllosilicate transition occurs at approximately the same depth as the breakdown of pumpellyite to epidote. Chlorite occurs in greenschist (or prehnite-actinolite) facies assemblages throughout the lower 1B lavas and the dike and sill complex.

The similarity between the zonation of phyllosilicates and calc-silicate minerals within the volcanic members of the Point Sal and Del Puerto remnants indicates that at least some portions of the California Coast Range ophiolite were more intensely hydrothermally altered than that of most oceanic crust and ophiolites studied to date. Volcanic units of the latter exhibit extensive submarine weathering or alteration to smectite and low-temperature zeolites and only rarely to mineral assemblages of the prehnite-pumpellyite facies. Phyllosilicates of the volcanic units of the Coast Range ophiolite are dominantly mixed-layered chlorite/smectite, indicating a higher temperature of alteration than that necessary for recrystallization to smectite and zeolites. Although the volcanic units of the Coast Range ophiolite manifest a higher grade of metamorphism than that found in other ophiolites and oceanic crust, the prehnite-actinolite facies assemblages from the dike complexes are generally the same: chlorite + quartz + epidote ± actinolite ± albite ± prehnite.

The observed phyllosilicate and calc-silicate mineral assemblages and zonations indicate a local thermal gradient in excess of 100 °C/km during the metamorphism of the Point Sal volcanic and dike members. High-variance mineral assemblages, ubiquitous in the lavas and dike rocks, reflect a high integrated fluid/rock ratio during metamorphic recrystallization. The zonation is characterized by relatively sharp mineral transitions characteristic of hydrothermal, low-pressure–low-temperature metamorphism.

Chlorite from mafic volcanic rocks in submarine hydrothermal systems generally does not have Si cation contents greater than 6.25 on the basis of 28 oxygens. Phyllosilicates of the Point Sal remnant, which plot within accepted chlorite compositional fields, are clearly mixed-layered chlorite/smectite and not chlorite. Therefore, low-temperature phyllosilicates should not be identified solely on the basis of compositional analysis; systematic X-ray diffraction analysis should be used to confirm the presence of chlorite, smectite, and mixed-layered phyllosilicates, within hydrothermally altered rocks.

Acknowledgments

We thank Cliff Hopson for his encouragement and support of this study. Lynn Whittig and Bill Allardice introduced L.A.B. to the practical techniques of phyllosilicate XRD. Howard Day, Lynn Whittig, J. G. Liou, Moonsup Cho, Doug McDowell, Rachel Haymon, and William Wise provided thorough reviews of various versions of this manuscript. Special thanks to Bill Wise for showing us his method of recalculating microprobe analyses of interlayered smectite/chlorite. This research was supported by NSF Grant 83-16544.

References cited

Alt, J.C., Laverne, C., and Muehlenbachs, K. (1985) Alteration of the upper oceanic crust: Mineralogy and processes in Deep Sea Drilling Project Hole 504B, Leg 83. In R.N. Anderson, J. Honnorez, K. Becker, et al., Eds., Initial reports of the Deep Sea Drilling Project, vol. 83, p. 217–247. U.S. Government Printing Office, Washington, D.C.

Alt, J.C., Honnorez, J., Laverne, C., and Emmermann, R. (1986) Hydrothermal alteration of a 1 km section through the upper oceanic crust, DSDP Hole 504B: Mineralogy, chemistry, and evolution of seawater-basalt interactions. Journal of Geophysical Research, 91, 10309–10335.

April, R.H. (1981) Trioctahedral smectite and interstratified chlorite/smectite in Jurassic strata of the Connecticut Valley. Clays and Clay Minerals, 29, 31–39.

Bailey, E.H., and Blake, M.C. (1974) Major chemical characteristics of Mesozoic Coast Range ophiolite in California. U.S. Geological Survey Journal of Research, 2, 637–656.

Bailey, E.H., Blake, M.C., and Jones, D.L. (1970) On-land Mesozoic oceanic crust in California Coast Ranges. U.S. Geological Survey Professional Paper 700-C, C70–C81.

Bass, M.N. (1976) Secondary minerals in oceanic basalt, with special reference to Leg 34, Deep Sea Drilling Project. In R.S. Yeats, S.R. Hart et al., Eds., Initial reports of the Deep Sea Drilling Project, vol. 34, p. 393–432. U.S. Government Printing Office, Washington, D.C.

Bettison, L. (1986) Authigenic phyllosilicate mineralogy of the Point Sal remnant, California Coast Range ophiolite. M.S. thesis, University of California, Davis, California.

Bird, D.K., Schiffman, P., Elders, W.A., Williams, A.E., and McDowell, S.D. (1984) Calc-silicate mineralization of active geothermal systems. Economic Geology, 79, 671–695.

Bischoff, J.L. (1980) Geothermal system at 21°N, East Pacific Rise: Physical limits on geothermal fluid and role of adiabatic expansion. Science, 207, 1465–1469.

Blake, M.C., and Jones, D.L. (1981) The Franciscan assemblage and related rocks in northern California: A reinterpretation. In W.E. Ernst, Ed., Geotectonic development of California, p. 308–328. Prentice-Hall, Englewood Cliffs, New Jersey.

Brown, G., and Brindley, G.W. (1980) X-ray diffraction procedures for clay mineral identification. In G.W. Brindley and G. Brown, Eds., Crystal structures of clay minerals and their X-ray identification, p. 305–360. Mineralogical Society, London.

Colby, J.W. (1968) Quantitative microprobe analysis of thin insulating films. In J. Newkirk, G. Mallet, and H. Pfeiffer, Eds., Advances in X-ray analysis, v. 11, p. 287–305.

Coleman, R.G. (1984) Preaccretion tectonics and metamorphism of ophiolites. Ofioliti, 9, 205–222.

Ellis, A.J. (1979) Explored geothermal systems. In H.L. Barnes, Ed., Geochemistry of hydrothermal ore deposits (2nd edition), p. 632–683. Wiley, New York.

Evarts, R.C. (1977) The geology and petrology of the Del Puerto ophiolite, Diablo Range, central California Coast Ranges. In R.G. Coleman and W.P. Irwin, Eds., North American ophiolites. Oregon Department of Geology and Mineral Industries Bulletin 95, 121–139.

Evarts, R., and Schiffman, P. (1983) Submarine hydrothermal metamorphism of the Del Puerto ophiolite, California. American Journal of Science, 283, 289–340.

Franzson, H., Gudmundsson, A., Fridleifsson, G.O., and Tomasson, J.

(1986) Nesjavellir high-T field, SW Iceland—Reservoir geology. Proceedings of the Fifth International Symposium on Water-Rock Interaction, 210–213.

Gillis, K.M., and Robinson, P.T. (1985) Low-temperature alteration of the extrusive sequence, Troodos ophiolite, Cyprus. Canadian Mineralogist, 23, 431–441.

Hauff, P.L. (1981) Corrensite: Mineralogical ambiguities and geologic significance. U.S. Geological Survey Open-File Report 81-85.

Hay, R.L. (1978) Geologic occurrence of zeolites. In L.B. San and F.A. Mumpton, Eds., Natural zeolites: Occurrence, properties, use, p. 135–143. Pergamon Press, Oxford.

Haymon, R.M., and Kastner, M. (1986) The formation of high temperature clay minerals from basalt alteration during hydrothermal discharge on the East Pacific Rise axis at 21°N. Geochimica et Cosmochimica Acta, 50, 1933–1939.

Hey, M.H. (1954) A new review of the chlorites. Mineralogical Magazine, 30, 272–292.

Hoffman, J., and Hower, J. (1979) Clay mineral assemblages as low-grade metamorphic geothermometers: Application to the thrust-faulted Disturbed Belt of Montana, U.S.A. In P.A. Scholle and P.R. Schluger, Eds., Aspects of diagenesis, p. 55–79. Society of Economic Paleontologists and Mineralogists Special Publication 26.

Hopson, C.A., and Frano, C.J. (1977) Igneous history of the Point Sal ophiolite, southern California. In R.G. Coleman and W.P. Irwin, Eds., North American ophiolites, p. 161–183. Oregon Department of Geology and Mineral Industries Bulletin 95.

Hopson, C.A., Frano, C.J., Pessagno, E.A., Jr., and Mattinson, J.M. (1975) Preliminary report and geologic guide to the Jurassic ophiolite near Point Sal, southern California coast. Geological Society of America Cordilleran Section Guidebook to Field Trip No. 5.

Hopson, C.A., Mattinson, J.M., and Pessagno, E.A. (1981) Coast Range ophiolite, western California. In W.G. Ernst, Ed., Geotectonic development of California, p. 419–510. Prentice-Hall, Englewood Cliffs, New Jersey.

Hower, J. (1981) X-ray diffraction identification of mixed-layer clay minerals. In F.J. Longstaffe, Ed., Clays and the resource geologist, p. 39–59. Mineralogical Association of Canada, v. 7.

Jackson, M.L. (1975) Soil chemical analysis—Advanced course (2nd edition). Published by the author. Department of Soil Science, University of Wisconsin, Madison, Wisconsin.

Keith, T.E.C., Mariner, R.H., Bargar, K.E., Evans, W.C., and Presser, T.S. (1984) Hydrothermal alteration in Oregon's Newberry volcano no. 2: Fluid chemistry and secondary-mineral distribution. Geothermal Resources Council Bulletin, 13, no. 4, 9–17.

Kristmannsdóttir, H. (1975) Clay minerals formed by hydrothermal alteration of basaltic rocks in Icelandic geothermal fields. Geologiska Föreningens i Stockholm Förhandlingar, 97, 289–292.

——— (1979) Alteration of basaltic rocks by hydrothermal activity at 100–300 °C. In M.M. Mortland and V.C. Farmer, Eds., International Clay Conference 1978. Elsevier, Amsterdam, Holland.

Liou, J.G. (1971) Analcime equilibria. Lithos, 4, 389–402.

Liou, J.G., Seki, Yotaro, Guillemette, R.N., and Saki, H. (1985) Compositions and parageneses of secondary minerals in the Onikobe geothermal system, Japan. Chemical Geology, 49, 1–20.

Liou, J.G., Maruyama, S., and Cho, M. (1987) Very low-grade metamorphism of volcanic and volcaniclastic rocks—Mineral assemblages and mineral facies. In M. Frey, Ed., Very low-grade metamorphism, p. 59–113. Blackie and Son, Ltd., Glasgow, Scotland.

Lippmann, F. (1954) Uber einen Keuperton von Zaisersweiher bei Maulbronn. Heidelberger Beitrage zur Mineralogie und Petrographie, 4, 130–134.

Moody, J. (1979) Serpentinites, spilites, and ophiolite metamorphism. Canadian Mineralogist, 17, 871–889.

Page, B.M. (1972) Oceanic crust and mantle fragment in subduction complex near San Luis Obispo, California. Geological Society of America Bulletin, 83, 957–972.

Pike, J.N. (1974) Intrusions and intrusive complexes in the San Luis Obispo ophiolite: A chemical and petrologic study. Ph.D. thesis. Stanford University, Stanford, California.

Pritchard, R.G. (1980) Alteration of basalts from Deep Sea Drilling Project Legs 51, 52, and 53, Holes 417A and 418A. In T. Donnely, J. Francheteau, W. Bryan et al., Eds., Initial reports of the Deep Sea Drilling Project, vol. 51–53, Part 2, p. 1185–1200. U.S. Government Printing Office, Washington, D.C.

Robinson, P., Flower, M.F.J., Schmincke, H.-U., and Ohnmacht, W. (1977) Low temperature alteration of oceanic basalts, DSDP Leg 37. In F. Aumento, W.G. Melson et al., Eds., Initial reports of the Deep Sea Drilling Project, vol. 37, p. 391–407. U.S. Government Printing Office, Washington, D.C.

Saleeby, J. (1981) Ocean floor accretion and volcano plutonic arc evolution of the Mesozoic Sierra Nevada. In W.G. Ernst, Ed., Geotectonic development of California, p. 132–181. Prentice-Hall, Englewood Cliffs, New Jersey.

Scheidegger, K.F., and Stakes, D.S. (1980) X-ray diffraction and chemical study of secondary minerals from Deep Sea Drilling Project, Leg 51, Holes 417A and 417D. In T. Donnely, J. Francheteau et al., Eds., Initial reports of the Deep Sea Drilling Project, vol. 51–53, Part 1, p. 1253–1263. U.S. Government Printing Office, Washington, D.C.

Schiffman, P., and Smith, B. (1988) Petrology and O-isotope geochemistry of a fossil seawater hydrothermal systems within the Solea graben, northern Troodos ophiolite, Cyprus. Journal of Geophysical Research, in press.

Schiffman, P., Williams, A.E., and Evarts, R.C. (1984) Oxygen isotope evidence for submarine hydrothermal alteration of the Del Puerto ophiolite, California. Earth and Planetary Science Letters, 70, 207–220.

Schiffman, P., Bettison, L., and Williams, A. (1986) Hydrothermal metamorphism of the Point Sal remnant, California Coast Range ophiolite. Proceedings of the Fifth International Symposium on Water-Rock interactions, 489–492.

Seki, Y., Liou, J.G., Guillemette, R., Sakai, H., Oki, Y., Hirano, T., and Onuki, H. (1983) Investigation of geothermal systems in Japan I. Onikobe Geothermal Area, Hydroscience and Geotechnology Laboratory, Saitama University, Memoir No. 3.

Seyfried, W.E., Jr. (1987) Experimental and theoretical constraints on hydrothermal alteration processes at mid-ocean ridges. Annual Review of Earth and Planetary Sciences, 15, 317–336.

Shervais, J.W., and Kimbrough, D.L. (1985) Geochemical evidence for the tectonic setting of the Coast Range ophiolite: A composite island arc–oceanic crust terrane in western California. Geology, 13, 35–38.

Środoń, J. (1980) Precise identification of illite/smectite interstratifications by X-ray powder diffraction. Clays and Clay Minerals, 28, 401–411.

Sucheki, R.K., Perry, E.A., and Hubert, J.F. (1977) Clay petrology of Cambro-Ordovician continental margin, Cow Head klippe, western Newfoundland. Clays and Clay Minerals, 25, 163–170.

Thompson, A.B. (1971a) Analcite-albite equilibria at low temperatures. American Journal of Science, 271, 79–92.

——— (1971b) P_{CO_2} in low grade metamorphism: Zeolite, carbonate, clay mineral prehnite relations in the system CaO-Al_2O-SiO_2-CO_2-H_2O. Contributions to Mineralogy and Petrology, 33, 145–161.

Velde, Bruce. (1977) A proposed phase diagram for illite, expanding chlorite, corrensite and illite-montmorillonite mixed layered minerals. Clays and Clay Minerals, 25, 264–270.

Walker, G.F. (1957) On the differentiation of vermiculites and smectites in clays. Clay Mineralogy Bulletin, 3, 154–163.

——— (1958) Reaction of expanding lattice minerals with glycerol and ethylene glycol. Clay Mineralogy Bulletin, 3, 302–313.

Zen, E-An. (1959) Clay mineral-carbonate relations in sedimentary rocks. American Journal of Science, 257, 29–43.

Zen, E-An, and Thompson, A.B. (1974) Low-grade metamorphism: Mineral equilibrium relations. Annual Reviews Earth and Planetary Science, 2, 179–212.

Manuscript received September 15, 1986
Manuscript accepted September 23, 1987